Diatom frustule photonic crystal geometric and optical characterization

Jonathan Mishler[a], Phillip Blake[b], Andrew J. Alverson[c], D. Keith Roper[b,d,e], Joseph B. Herzog[*,a,d,e]

[a]Department of Physics, University of Arkansas, Fayetteville, AR, USA 72701;
[b]Ralph E. Martin Dept. of Chemical Engineering, Univ. of Arkansas, Fayetteville, AR, USA 72701;
[c]Department of Biological Sciences, University of Arkansas, Fayetteville, AR, USA 72701;
[d]Microelectronics-Photonics Program, University of Arkansas, Fayetteville, AR, 72701, USA;
[e]Institute for Nanoscience and Engineering, University of Arkansas, Fayetteville, AR 72701, USA

ABSTRACT

Diatom algae are single-celled, photosynthetic organisms with a cell wall called a frustule—a periodically patterned nano-structure made of silica. Throughout the last decade, diatom frustules have been studied for their potential uses as photonic crystals and biomimetic templates for artificially developed metamaterials. A MATLAB program characterizing their pore structure as a function of angle was developed, potentially giving insight into how their geometric characteristics determine their optical properties.

Keywords: Diatoms, photonic crystal, geometric structure analysis, nano biophotonics, biomimetics, nanotechnology

1. INTRODUCTION

Photonic crystals are periodically patterned dielectric nanostructures that can direct the motion of light belonging to certain optical bandwidths. The periodicity of the nanostructure determines which bands of light can pass through the material, and which are directed around the photonic crystal. Applications of photonic crystals include thin-film optics[1], photonic-crystal fibers[2], photon-state squeezing[3], micro-fabricated lasers[4], and optical computers[5]. As fabrication techniques advance, the number of applications exploiting photonic crystals will grow.

The silicified cell walls, or frustules, of diatom algae represent a naturally occurring photonic crystal that has been studied for its optical properties[6]. Different species of diatoms have frustules with different shapes, periodicities, and patterns, giving each species unique optical properties. Diatom frustules have already been used as biomimetic photonic crystals, in which a replica mold of the frustule is created with polydimethylsioloxane[7]. Using specialized lab techniques, diatoms have also been grown with frustules made of materials other than silica with controlled patterns[8,9]. These capabilities make diatom frustules of interest to the field of nanophotonics. Figure 1 shows an image taken with a scanning electron microscope (SEM) of a marine diatom species.

The diatom lineage dates to roughly 200 million years ago[10], allowing ample time for evolution to refine their physical characteristics and select for different optical properties. A new diatom pore characterization using MATLAB code is reported. This MATLAB code is built upon existing code developed for other purposes[11]. The goal of this characterization is to understand how diatom pore geometries influence their optical properties. By understanding this correlation, diatoms can serve as biomimetic templates for artificially developed photonic crystals with desirable optical properties.

* Email: jbherzog@uark.edu

Nanobiosystems: Processing, Characterization, and Applications VII, edited by Norihisa Kobayashi, Fahima Ouchen, Ileana Rau, Proc. of SPIE Vol. 9171, 91710P · © 2014 SPIE · CCC code: 0277-786X/14/$18 · doi: 10.1117/12.2062287

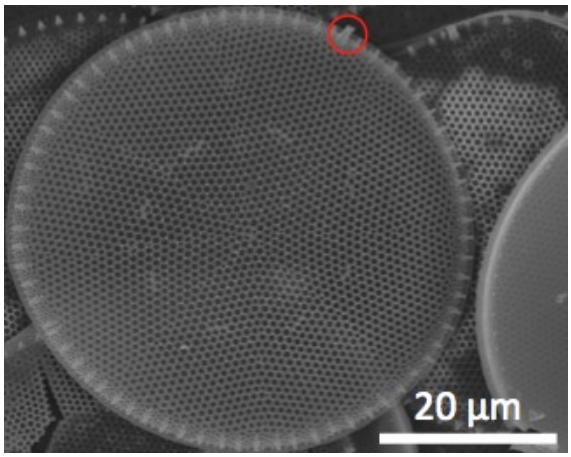

Figure 1. Scanning electron micrographs of marine diatom, *Thalassiosira anguste-lineata*. Circled, is the labiate process. This is a single fixed point of asymmetry on the diatom frustule. It is a useful point of reference when considering symmetries present in frustules.

2. MATLAB CODE

This work characterized a single diatom frustule of the marine diatom, *Thalassiosira anguste-lineata*, shown in Figure 1 and 2A. A single diatom pore shown in Figure 2B illustrates how the characterization works. To begin, the image is uploaded into MATLAB and is converted into a matrix containing the image data. The length of the scale bar and the number of pixels contained within the scale bar are also input into the function to convert from pixel length to physical length. Using this matrix, the image is converted into a binary image, as shown in Figure 2C. The MATLAB function then determines the perimeter, centroid, coordinates, and area of the pore using built-in functions. The program then calculates the radius of a circle whose area is equivalent to the area of the pore using the formula,

$$r = \sqrt{\frac{A}{\pi}}$$

whereby A is the area of the pore, similar to the algorithm in [11]. Here r is called the effective radius of the pore. Next, as illustrated in Figure 2D, the difference between the radius of the pore and the radius of the circle (Δr) is computed as a function of the angle. The data are then filtered using a built-in MATLAB Savitsky–Golay filter. These data are normalized relative to the effective radius and plotted in Cartesian coordinates, as illustrated in Figure 2E.

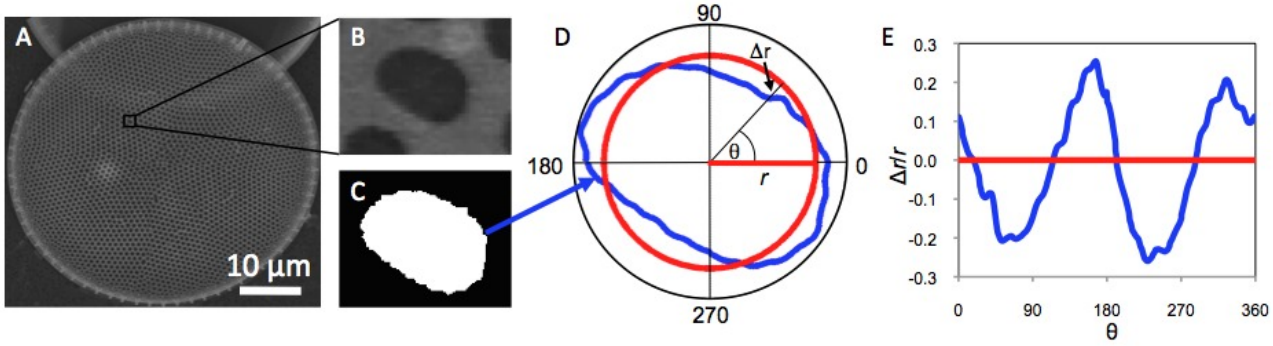

Figure 2. (A) SEM of diatom species *Thalassiosira anguste-lineata*. (B) Single diatom pore. (C) Binary image of single diatom pore. (D) Polar plot of perimeter of diatom pore relative to a circle with an equivalent area. (E) Normalized Cartesian plot of Δr vs. θ.

3. DIATOM PORE CHARACTERIZATION

As seen in Figure 2A, the diatom is resting on another diatom. This can potentially skew the image and make the pores appear to be more elliptical than they are. Additionally, high-resolution SEM images can be slow and can sometimes also skew images significantly in the vertical directions. To compensate for both of these, the image was vertically stretched to make the diatom circular. Since the diatom images are relatively small and the program works with pixels, the image was also diagonally stretched by a factor of 10 to minimize any error that may arise from an insufficient number of pixels to accurately represent the pores. The scale bar shown in Figure 2A was also scaled by a factor of 10, increasing the number of pixels it contains.

Pores from the stretched and scaled image were analyzed by the program, which calculated the effective radius, centroid, coordinates, and area of each pore. Figure 3A shows a histogram of the effective radii of the pores, which had an average effective radius of approximately 331 nm. As there are thousands of pores on the diatom surface, simply plotting Δr vs. θ for each pore on the same plot is not an effective way to represent the data since it is impossible to determine regions of higher point density. Instead, a pseudocolor plot shown in Figure 3B was used to show the superposition of plots of Δr vs. θ. In this plot, the brighter regions indicate a higher point density. To create this plot, the program first partitions θ into bins with a size of 1 degree. The program then counts the number of points of Δr contained in each bin. Next, for each bin of θ, the program partitions Δr into bins. The number of points contained within these bins is then calculated, and the bin matrix is converted into a pseudocolor plot with built-in MATLAB functions. This plot is essentially a 2D histogram: a collection of 1D histograms of Δr for each bin of θ.

A 1D histogram of Δr integrated over all angles was created and is shown in Figure 3C. This histogram reveals that most values of Δr are close to 0 nm, as expected, and the standard deviation of Δr of the pores is approximately 16.6 nm.

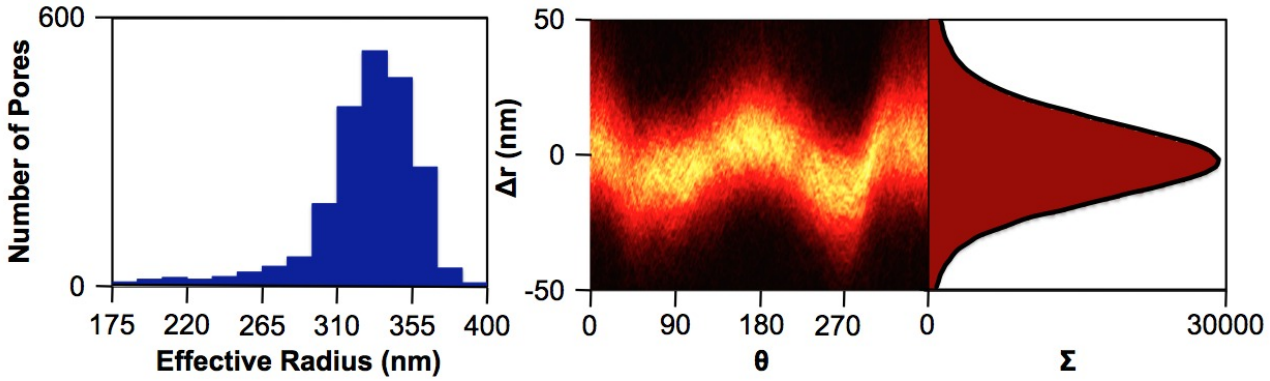

Figure 3. (A) Histogram of effective radii of pores from diatom of Figure 1. (B) 2D Histogram pseudocolor plot of superimposed plots of Δr vs. θ for each diatom pore. Brighter regions indicate higher point density. (C) Histogram of Δr integrated over θ. The black line is a Gaussian fit that determined the standard deviation of Δr to be approximately 16.6 nm.

Observe that in Figure 1, faint lines divide the diatom into 8 sectors with similar areas. To reveal any pore symmetries present in the diatom, the sectors were separated from each other and analyzed individually by the program. These are presented in Figure 4, and the Δr 2D histogram as a function of θ has been created for each sector. The plot revealed several interesting symmetries. First, observe the symmetry between the first four sectors to the left of the labiate process (sectors I – IV), and the first four sectors to the right of the labiate process (sectors V – VIII). The pseudocolor plots of sectors I - IV appear to be continued by the pseudocolor plots of their sectors symmetric to the labiate process. Also notice that there are four sectors in which the Δr values are generally constant as a function of θ, whereas the other four sectors resemble cosine curves. It is interesting to point out that the sectors seem to exist in alternating pairs, where each pair has pores whose Δr values are either constant or resemble cosine curves. For instance, going clockwise, sectors I and V are a pair with pores whose Δr values are constant, while sectors VI and VII are a pair with pores whose Δr values resemble cosine curves. As shown, the pairs continue to alternate for the remainder of the sectors. However, it is important to mention that without examining other images of diatoms, drawing conclusions is problematic. Keeping this in mind, these patterns suggest a potentially important relationship.

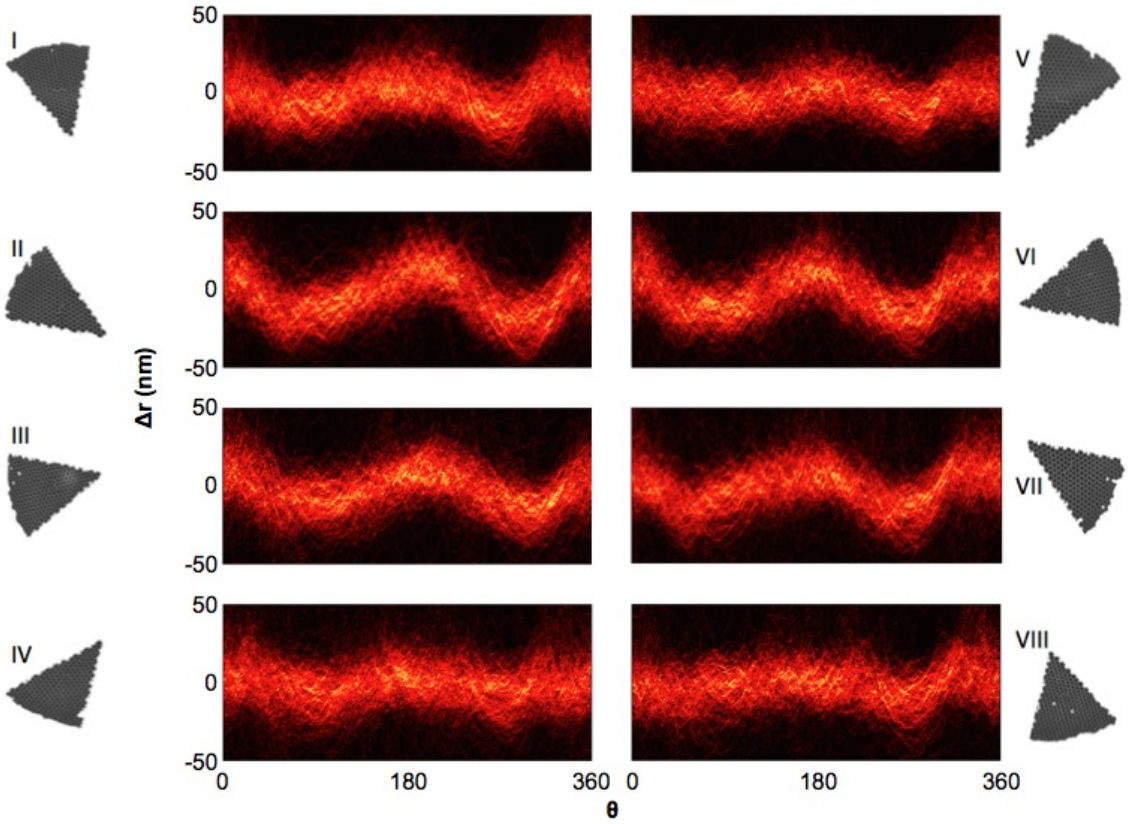

Figure 4. (I – VIII) Pseudocolor plots of superimposed plots of Δr vs. θ for each diatom pore by each diatom sector. Brighter regions indicate higher point density.

4. CONCLUSIONS

At a glance, the diatom pores of *Thalassiosira anguste-lineata* appear to have slightly elliptical shapes. The degree of ellipticity appears to be dependent on the location of the pores. On average, most values of Δr are concentrated between approximately –20 and 20 nm with a greater density at approximately 0 nm, which is consistent with the standard deviation of 16.6 nm.

5. FUTURE WORK

More diatom species and images need to be analyzed to draw any conclusions about the pore symmetries of diatom cell walls. In addition to analyzing more diatom images, the diatom pore geometries can be input into COMSOL multiphysics using the MATLAB code to model their optical properties and potential photonic crystal behavior. By comparing these COMSOL simulations to existing simulations of artificially designed photonic crystals, it may be possible to determine the influence of diatom pore geometries on their optical properties.

ACKNOWLEDGEMENTS

JM would like to acknowledge Laura Velasco for her support in this project. He also would like to acknowledge the Arkansas Department of Higher Education for funding his research through the Student Undergraduate Research Fellowship 2014, the Honors College at the University of Arkansas for travel funding, and SPIE for their travel funding. Additional research funding has been provided to JBH by the Department of Physics, the Fulbright College of Arts and Sciences, the Vice Provost for Research and Economic Development at the University of Arkansas, and the Honors College Mentor Award at the University of Arkansas.

REFERENCES

[1] Bermel, Peter et al., "Improving thin-film crystalline silicon solar cell efficiencies with photonic crystals" *Optics Express*, Vol. 15, Issue 25, pp. 16986-17000 (2007).

[2] Dudley, John M. et al., "Supercontinuum generation in photonic crystal fiber" *Rev. Mod. Phys.*, Vol.78, Issue 4, pp. 1135-1184 (2006).

[3] M. Banaee and J. Young, "Squeezed state generation in photonic crystal microcavities," Opt. Express **16**, 20908-20919 (2008).

[4] Izeikis, V., Matsuo, S., Juodkazis, S. and Misawa, H. (2006) [Femtosecond Laser Microfabrication of Photonic Crystals, in 3D Laser Microfabrication: Principles and Applications] (eds H. Misawa and S. Juodkazis), Wiley-VCH Verlag GmbH & Co. KGaA, Weinheim, FRG.

[5] Ouellette, J., "Seeing the Future in Photonic Crystals," Industrial Physicist, Vol. 7, No. 6, pp. 14-17, 2001.

[6] Fuhrmann, T., Landwehr, S., El Rharbi-Kucki, M. and Sumper, M., "Diatoms as living photonic crystals", *Applied Physics B: Lasers and Optics* **78**, 257-260 (2004).

[7] Hlúbiková, D., A. T. Luís, V. Vaché, L. Ector, L. Hoffmann, and P. Choquet. "Optimization of the Replica Molding Process of PDMS Using Pennate Diatoms." *Journal of Micromechanics and Microengineering* 22.12: (2012).

[8] Rorrer, G. L. "Biosynthesis of Silicon-germanium Oxide Nanocomposites by the Marine Diatom Nitzschia Frustulum." *Journal of Nanoscience and Nanotechnology* 5.1: 41-49 (2005).

[9] Losic, Dusan, Gerry Triani, Peter J. Evans, Armand Atanacio, James G. Mitchell, and Nicolas H. Voelcker. "Controlled Pore Structure Modification of Diatoms by Atomic Layer Deposition of TiO2." *Journal of Materials Chemistry* 16.41: 4029 (2006).

[10] Ulf Sorhannus, "A nuclear-encoded small-subunit ribosomal RNA timescale for diatom evolution, Marine Micropaleontology", Volume 65, Issues 1–2, 29 October 2007, Pages 1-12

[11] P. Blake, W. Ahn, and D.K. Roper, "Enhanced uniformity in arrays of electroless plated spherical gold nanoparticles using tin presensitization," *Langmuir*